Design and implementation of distribution-free Phase-II charting schemes based on unconditional run-length percentiles

Jean-Claude Malela-Majika[a] and Marien A. Graham[b]

[a]Department of Statistics, Faculty of Natural and Agricultural Sciences, University of Pretoria, Hatfield, South Africa Pretoria; [b]Department of Science, Mathematics and Technology Education, University of Pretoria, Pretoria, South Africa

ABSTRACT

Traditionally, the mean of the run-length distribution (*ARL*) of an in-control (IC) process is used to design and implement statistical process charting schemes. When standards are unknown (Case U), the unconditional *ARL* is considered during Phase-II monitoring—surprisingly, by suppressing the term "unconditional." The literature has recently highlighted the difference between the unconditional and the conditional *ARL* in studying the properties of Phase-II charting schemes under the Case U. The effects of bias in the Phase-I sample may lead to remarkably high rates of early false alarms. We explore the idea of restricting the probability of unconditional early false alarms by using lower percentile points of the unconditional run-length distribution to design nonparametric charting schemes. This new approach is named "the lower percentile-based (LPL) design." We consider the design and implementation of six distribution-free schemes: five precedence-type schemes and the rank-sum scheme. We carry out simulations to compare the six schemes with a prefixed value of some lower percentile point of the IC run-length distribution. The best scheme is the one with the lowest value for a specific higher percentile point of the out-of-control run-length distribution. We illustrate the new design and implementation strategies with real data, and offer a summary and concluding remarks.

ARTICLE HISTORY
Received 10 July 2020
Accepted 10 May 2022

KEYWORDS
Distribution-free monitoring scheme; false alarm probabilities; lower percentile-based approach; Phase-I bias; precedence-type monitoring schemes; rank-sum monitoring scheme

1. Introduction

From health care surveillance (e.g., Chen and Huang 2014; Li and Qiu 2016) to maintaining service quality (e.g., Mukherjee and Sen 2018), from the sequential investigation of environmental pollution (e.g., Čampulová, Veselík, and Michálek 2017) to ensuring product quality (e.g., Li, Liu and Xian 2017; Song, Mukherjee, Liu and Zhang 2019), or monitoring social networks (e.g., Woodall, Zhao, Paynabar, Sparks and Wilson 2017), Phase-II process charting schemes are one of the most popular statistical tools. Practitioners often implement a Phase-II charting scheme on the assumption that that the process parameters are known (Case K). However, in practice, process parameters

CONTACT Marien A. Graham marien.graham@up.ac.za Department of Science, Mathematics and Technology Education, University of Pretoria, Pretoria, South Africa.

are typically estimated (i.e., Case U) from a presumably in-control (IC) Phase-I reference sample. Many studies have established that the Phase-II charting schemes under the Case U suffer from estimation bias. As a result, their IC performance often becomes worse owing to the increased chance of false alarms; see, for example, the well-known article by Jensen, Jones-Farmer, Champ and Woodall (2006).

A common practice when implementing charting schemes under the Case K and Case U is to employ some standard metrics such as the average run-length (*ARL*) or the median run-length (*MRL*). See, for example, Chakraborti (2007) and Kumar and Baranwal (2019) for more details on appropriate performance metrics. As a consequence, false alarms are often too high for most of the charting schemes under Case U. For example, if we set the IC *ARL* (say, ARL_0) of the traditional Shewhart $\overline{X}$ chart for a normally distributed process at 500, it has a false alarm rate (*FAR*) of 0.002, and the cumulative probability of false alarms (*CPFA*) until the 25th sample is about 4.88%; readers can easily verify this using the geometric run-length property of the traditional Shewhart $\overline{X}$ chart. On the other hand, the run-length distribution of Phase-II charting schemes under the Case U is only conditionally geometric, given a Phase-I sample. Thus, the *CPFA* represents the cumulative probability that there will be a false alarm on or before a pre-specified number of test samples (denoted as ϑ), which we write as $P(N \le \vartheta)$ where N represents the run-length random variable. Suppose that $\pi(\vartheta)$ is the unconditional *CPFA* (*UCPFA*) of boundary-crossing on or before the test sample ϑ, and that $\pi(\vartheta|IC)$ (denoted as $\pi_0(\vartheta)$) is the *UCPFA* for the IC case. In most cases, for charting schemes under the Case U, $\pi_0(25)$ is usually much higher than 4.88%.

In this article, motivated by Faraz, Saniga and Montgomery (2019), we explore a percentile-based implementation design for a class of Phase-II distribution-free charting schemes under the Case U. All the schemes considered in this article are nonparametric, as nonparametric charts hold many advantages over parametric charts. For a detailed overview of nonparametric charts, we refer the reader to Chakraborti and Graham (2019a, 2019b). First, consider the case where we implement a popular Phase-II Shewhart-type distribution-free scheme based on the Wilcoxon rank-sum (WRS) statistic by setting $ARL_0 = 500$. In such a case, the $\pi_0(25)$ is 20.2% when the reference sample size (say, m) is 30, and the test sample size (say, n) is 5; see Table 3 of Mukherjee and Sen (2015) for more details. They also noted that this problem becomes even more complicated when n increases, and that the problem only subdues as m increases. For example, for $m = 100$ and $n = 5$, the probability (i.e., $\pi_0(25)$) is 8.4%; and for $m = 1000$ and $n = 5$, this probability stabilizes at 4.82%. Likewise, if the Phase-I sample size is less than 30 in a Case U set-up, most of the existing Phase-II distribution-free charting schemes are practically inadmissible. The problem arises, however, from the fact that researchers and practitioners are often too excited about setting the ARL_0 at 500 or some other acceptable standard, instead of focusing on restricting too many early false alarms.

In this article, we propose a percentile-based design and implementation scheme in the following way:

1. Set $\pi_{0s}(\vartheta)$ at a low prefixed level, say $\gamma \in (0,1)$, for the s^{th} scheme ($s = 1, 2..., S$). This is equivalent to setting the $100\gamma^{th}$ IC run-length percentile at

ϑ (a condition that can be used as a metric to determine the control limit(s) and to restrict the probability of early false alarms). When the metric is the IC *MRL*, $\gamma = 0.5$.

But consistent with classical testing, we suggest using a smaller γ, say, $\gamma \in (0, 0.1)$. Since the run-length distribution is discrete, we often observe jumps, and in practice one may not get control limits that exactly yield $\pi_{0s}\ (\vartheta) = \gamma$. In such cases, we recommend choosing the closest value; that is, $\pi_{0s}\ (\vartheta) \approx \gamma$. Repeat this for various competitive schemes to protect against too many early false alarms.

2. We choose the best plan from among various competing charting schemes—one that quickly detects a correct signal with a very high unconditional cumulative probability. This is equivalent to comparing several schemes based on a higher-order OOC run-length percentile, which is usually much higher than the traditional choice of the median.

Suppose that the $100\tau^{th}$ OOC run-length percentile of the s^{th} scheme under a shift δ is $R_{\delta s}$, given $\pi_{0s}\ (\vartheta) \approx \gamma$. If $\pi_\delta\ (R_{\delta s})$ denotes the *UCP* of an actual signal under a shift δ until test sample $R_{\delta s}$, given $\pi_{0s}\ (\vartheta) \approx \gamma$, we have $\pi_\delta(R_{\delta s}) = \tau$. Note that, in OOC-*MRL* based comparisons, we use $\tau = 0.5$; but, to achieve higher power of the control charts, we recommend a higher value of τ, say $\tau \in [0.9, 1)$. Now the best scheme (i.e. S^* for any $S^* \in \{1, 2, ..., S\}$) is obtained such that

$$UCP = \pi_\delta\ (R_{\delta s})\ \ = P(N \leq R_{\delta s} \mid \delta \neq 0)$$

and

$$R_{\delta S^*} = \min\{R_{\delta s}; s = 1, 2, ..., \ S\}.$$

where $R_{\delta S^*}$ is the number of test samples corresponding to the charting scheme S^*.

Chakraborti, Laan and Wiel (2004) considered a class of Shewhart-type distribution-free precedence charting schemes that have the advantage of having the same IC run-length distribution for all continuous process distributions. They derived exact expressions for the run-length distribution and the *ARL*, and studied the schemes' characteristics by evaluating the run-length distribution probabilities and the *ARL*. They provided results for the implementation of such schemes along with IC robustness characteristics. Graham, Mukherjee and Chakraborti (2012) and Mukherjee, Graham and Chakraborti (2013) extended the idea to construct EWMA and CUSUM-type schemes, based on a similar pivot. For more recent work involving precedence schemes, we refer the reader to Malela-Majika et al. (2020) and Malela-Majika, Shongwe, and Castagliola (2022).

Precedence-type schemes mostly use notions of precedence tests. Balakrishnan and Ng (2006) outlined the masking effect of ordinary precedence tests. We find similar problems in precedence-type charting schemes, and so their impacts need to be studied thoroughly. Balakrishnan, Paroissin and Turlot (2015) studied the properties of one-sided charting schemes based on precedence and weighted precedence statistics to detect small shifts. Maximal precedence tests and weighted maximal precedence tests are often found to be more potent than ordinary precedence tests in certain situations. Consequently, it is worth studying charting schemes that are based on maximal and weighted maximal precedence statistics. For an extensive discussion of some of these charting statistics, we recommend Koutras and Triantafyllou (2020).

The remainder of this paper is organized as follows: we introduce the statistical framework of the weighted and unweighted precedence-type charting schemes in Section 2. We present the lower percentile-based (LPL) design, implementation, and performance of various schemes with restricted *FAR* in Section 3. In Section 4, we give a real-life example of the application of the LPL schemes. We investigate the effect of the Phase-I bias in Section 5. In Section 6, we provide a summary and some recommendations. For simplicity, we only consider upper one-sided charting schemes that are used to detect an upward shift in the location parameter. In the illustrative example, we outline another justification for using upper one-sided control charts.

2. Some precedence-type tests and charting schemes

In this section, we revisit some distribution-free schemes that are based on ranking and precedence-type statistics.

2.1. Traditional precedence-type test and charting scheme

The precedence test is a distribution-free two-sample test based on the orders of early failures, initially introduced to compare the lifetimes of two populations. Many researchers have studied the precedence test's power properties; see, for instance, Chakraborti, Laan, and Wiel (2004) and Van der Laan and Chakraborti (2001). Let a random sample of m observations, say $X_1,\ X_2, \ldots,\ X_m,$ be available from an unknown continuous cumulative distribution function (cdf) $F_X(x)$. Also, consider a random sample of size $n,$ say $Y_1,\ Y_2, \ldots,\ Y_n,$ from an unknown continuous cdf $G_Y(y),$ for which we assume $G_Y(x) = F_X(x-\delta),$ where $\delta \in \mathbb{R}$ is the shift in the location parameter.

In a SPM set-up, $\delta = 0$ refers to an IC state. Define the precedence statistic W_j as the number of X-observations that precede $Y_{(j:n)}$. When $F = G,$ the exact probability distribution of the joint precedence statistic can be obtained by using combinatorial techniques (see Chakraborti, Laan, and Wiel 2004). The probability mass function (pmf) is given by

$$P_{IC}(W_j = w) = \frac{\binom{j+w-1}{w}\binom{m+n-j-w}{m-w}}{\binom{m+n}{m}}\ , \tag{1}$$

where $w = 0,\ 1, \ldots, m$.

It is easy to see that the IC distribution of W_j involves only $m,\ n,\ j$ and w. The pmf does not depend on the parent process distribution or parameters. Therefore, the decision rules based on W_j are distribution-free until the underlying distributions are continuous and identical.

The design of a distribution-free scheme for the sequential monitoring of location shift using a precedence statistic is simple. To this end, we consider the m observations, $X_1,\ X_2, \ldots,\ X_m,$ as the reference sample from an IC population (Phase-I sample). Further, we regard the h^{th} test sample or the Phase-II observations as $Y_{h1},\ Y_{h2}, \ldots,\ Y_{hn}$

of size n, where $h = 1, 2, 3, \ldots$. The Phase-II samples are drawn independently of one another and of the reference sample. Now arrange $X_1, X_2, \ldots, X_m$ in ascending order, and select two order statistics, $X_{(a:m)}$ and $X_{(b:m)}$, for some $1 \leq a < b \leq m$. The two-sided exceedance-/precedence-type charting scheme, as in Chakraborti, Laan, and Wiel (2004), has a lower control limit $(LCL) = X_{(a:m)}$ and an upper control limit $(UCL) = X_{(b:m)}$.

Two types of precedence schemes are popular in the literature. One is based on the number of reference sample observations; W_{jh} precedes the median of the h^{th} test sample. When n is an odd number, say $n = 2r + 1$—r is a positive integer, and $j = r + 1$. This is popularly known as the traditional precedence scheme, and is also called "the median scheme," which we abbreviate as the "Med" scheme. We plot the statistic as $W_{(r+1)h}$ against UCL, say b_{Med}, and declare that the process is OOC at the h^{th} test sample, and expect that there would be an upward shift in location if $W_{(r+1)h} \geq b_{Med}$. Otherwise, we regard the process as IC, and we move on to collect the next test sample. If the test sample size is even, say $j = 2r$, one can, without loss of generality, consider the number of reference sample observations preceding the average of the two middlemost observations of the h^{th} test sample, and denote the plotting statistic as $W_{\left(r+\frac{1}{2}\right)h}$.

We also consider another well-known precedence scheme that is based on the number of reference sample observations, in which W_{1h} precedes the minimum, that is $Y_{(1:n)}$, of the h^{th} test sample. This is popularly known as the "Min" scheme. The process is IC when W_{1h} plots below the UCL, say b_{Min}; otherwise it is OOC.

2.2. General maximal precedence test and charting scheme

When observing only a few early failures, a precedence test can determine a location difference under a life-test. This makes it cost-effective, since most life tests involve products that are destructive and expensive (Ng and Balakrishnan 2005). However, Balakrishnan and Frattina (2000) and Ng and Balakrishnan (2005), among others, have noted that the precedence test suffers from a "masking effect." The precedence test uses the sum of the frequency of failures from the X-sample, between the first j failures of the Y-sample. The masking effect comes from the fact that it ignores the distribution of this frequency of failures.

Balakrishnan and Frattina (2000) and Balakrishnan and Ng (2001) introduced the maximal precedence test, which can correct the problem of masking. In this case, the test statistic is not the number of failures that precede the j^{th} Y-failure. Rather, it is the maximum of the number of X-failures before the first Y-failure, between the first and second, and so on, until between the $(j-1)^{th}$ and j^{th} Y-failures. Suppose that there are U_1 failures before the first Y-failure, U_2 failures between the first and second Y-failures, $\ldots$, U_j failures between the $(j-1)^{th}$ and j^{th} Y-failures.

Figure 1 illustrates an example with $U_1 = 0$, $U_2 = 2$, $U_3 = 4$ and $U_4 = 1$. Note that we write the ordinary precedence statistic as

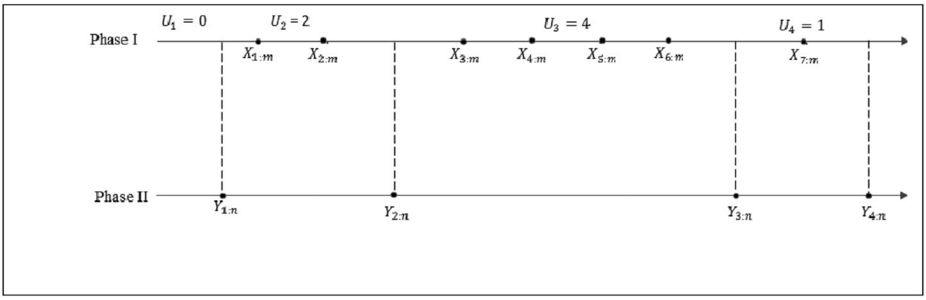

Figure 1. Illustration of U_i values.

$$W_j \equiv W_{Pre_j} = \sum_{k=1}^{j} U_k, \tag{2}$$

where the information given by $j \geq 3$ is masked. We define the general maximum precedence statistics as

$$W_{MPre_j} = Max\ (U_1\ ,\ ...,\ U_j). \tag{3}$$

The maximum precedence statistic circumvents the masking effect. In our example, the precedence statistic is given by $W_{pre_4} = \sum_{k=1}^{4} U_k = U_1 + U_2 + U_3 + U_4 = 0 + 2 + 4 + 1 = 7,$ and the maximum precedence statistic is given by $W_{MPre_4} = Max\ (0,\ 2,\ 4,\ 1) = 4$. We explore a charting scheme based on W_{MPre_j} in the current investigation, and refer to it as a maximal precedence-type scheme, abbreviated as the "M-Pre" scheme. Let $W_{MPre_j,h}$ be the plotting statistic of the M-Pre scheme, based on the reference sample and on the h^{th} Phase-II sample. The process is declared OOC when $W_{MPre_j,h}$ plots above the UCL, say b_{MPre}, where $1 \leq b_{MPre} < m$. Otherwise, we consider the process IC and collect the next test sample. For brevity, we only consider up to the median of the test sample. That is, we set $j = r + 1$ when $n = 2r + 1$, although one may set various other j, $1 \leq j \leq n$. Nevertheless, if $j = 1$, it boils down to the Min scheme, as in Section 2.1.

2.3. Weighted precedence-type statistics and charting schemes

Ng and Balakrishnan (2005) considered the weighted precedence-type tests, and assigned a decreasing weight to the number of earlier failures, U_j, as j increases. In our notation, the simple weighted precedence statistic, say W_{WPre_j} is

$$W_{WPre_j} = \sum_{k=1}^{j} (n - k + 1) U_k \tag{4}$$

and the weighted maximal precedence statistic, say W_{WMPre_j}, is

$$W_{WMPre_j} = \underset{1 \leq k \leq j}{\text{Max}} \{(n - k + 1) U_k\}. \tag{5}$$

We design the two charting schemes using W_{WPre_j} and W_{WMPre_j}. The plotting statistic, based on the reference sample and the h^{th} test sample of the weighted precedence scheme (say, W-Pre scheme), is $W_{WPre_j,h}$. We observe an OOC signal if $W_{WPre_j,h} >$

b_{WPre}, where b_{WPre} is the appropriate UCL. Similarly, the plotting statistic based on the reference sample and the h^{th} test sample of the weighted maximal precedence scheme (say, WM-Pre scheme) is $W_{WMPre_j,h}$. We observe an OOC signal if $W_{WMPre_j,h} > b_{WMPre}$, where b_{WMPre} is the appropriate UCL. As in Section 2.2, we consider only $j = r + 1$ when $n = 2r + 1$, although one may set various other j, $1 \le j \le n$.

In the next section, we discuss the percentile-based implementation techniques and design plans of the precedence-type schemes and the Shewhart rank-sum scheme.

3. Implementation and performance of various LPL charting schemes

Recall that this paper's main aim is to prefix the lower percentile point of the IC run-length distribution at some desired level, and to compare various schemes using a certain higher percentile point of the OOC run-length distribution. The best scheme, from among numerous competitors, is the one with the lowest value for a specific higher percentile point of the OOC run-length distribution. In the Section 1, we learnt that the run-length distribution follows a geometric probability model with a success probability of $p = 0.002$; the ARL_0 equals 500, and will occasionally produce false alarms. In that case, the fifth percentile point of the same run-length distribution is 25.62. Therefore, we observe close to a 5% chance that there will be a false alarm before the inspection of the 26th test sample. In the framework of the Shewhart $\overline{X}$ chart, setting $ARL_0 = 500$ is equivalent to setting the fifth percentile point at 25.62 or setting the first percentile point at 5.02. Similarly, setting $ARL_0 = 370$ is comparable with setting the fifth percentile point at 18.96 or setting the first percentile point at 3.72. The conditional run-length distribution of Phase-II Shewhart precedence type or rank-sum schemes, given the reference sample, is geometric, but the unconditional run-length distribution is complicated.

Along the same line of thinking, we propose implementing various schemes, as discussed in Section 2, by setting the fifth percentile point at 20 or 25, as the case may be. To control the FAR to a greater extent, one may consider setting the first percentile point of the run-length (PRL) value as 5 or 10, or the fifth percentile point as 50. Moreover, when $m = 100$, $n = 5$, and the target ARL_0 is 500, we observe 5% false alarms on or before the 16th test sample when we employ the Shewhart rank-sum scheme for the Phase-II monitoring of charting schemes under the Case U. In the same setting, we observe 5% false alarms on or before the 13th test sample if we use the Shewhart Med scheme. The situation becomes worse for both schemes when n increases. Setting the fifth percentile point at 20 or 25 will prevent early false alarms. It is easy to note that the attained ARL_0 will be more than 500 in all such cases; and so, the LPL procedure will maintain the current industry standard. For the Phase-II monitoring of charting schemes under the Case U, it is more important to prevent too many early false alarms rather than to set the target ARL_0 at a fixed level. Therefore, it is legitimate to design a charting scheme by setting a lower percentile point of the IC run-length distribution at a prefixed value. Thus, in this paper, we determine the charting constants by setting $\pi_0(\vartheta) = 0.05$, for $\vartheta = 20$, 25 and 50.

It may be reasonable to compare the 95th percentile point of the OOC run-length distribution of a class of charting schemes that are competing among themselves. We identify one with the smallest 95th OOC *PRL* value as the best scheme. That is, we set $\tau = 0.95$ to compute and compare $R_{\delta s}$ for various schemes. Next, we discuss the implementation steps of the upper one-sided unweighted and weighted maximum precedence-type charting schemes.

3.1. Implementation steps

We adopt the following steps to implement all the schemes described in Section 2:

1. Specify the Phase-I reference sample size (m) and the Phase-II test sample size (n).
2. Set $(\vartheta,\ \gamma)$, for example, $(\vartheta = 25,\ \gamma = 0.05)$, and determine the *UCL* for various schemes, as explained in Subsection 3.2.
3. Observe and establish a Phase-I (reference) sample, $\boldsymbol{X}_m = \{X_1, X_2, ..., X_m\}$, of size m from the IC process.
4. Collect the test sample, $\boldsymbol{Y}_{\boldsymbol{hj}} = \{Y_{h1},\ Y_{h2}, ..., Y_{hn}\}$, where $h = 1,\ 2,\ 3,\ \dots$ and $j = 1,\ 2,\ \dots,\ n$, during the h^{th} stage of Phase-II monitoring.
5. Calculate the appropriate charting statistic and plot it against the corresponding *UCL*, as indicated in Section 2.
6. During the Phase-II monitoring, if the h^{th} plotting statistic exceeds the corresponding *UCL*, the process is OOC at the h^{th} test sample. Otherwise, the process is IC, and monitoring continues with the next test sample.

We need to determine the *UCL* values of various schemes to implement these schemes properly. Next, we discuss the search algorithm to determine *UCL* values.

3.2. Determination of the control limit constant

It is easy to note that the control limits b_{Med} or b_{Min} of the traditional precedence-type charting scheme, based on the median of the reference sample or the minimum order statistic of the Phase-II sample, are, in fact, integers between 1 and m. Similarly, the control limit for the maximal precedence scheme, that is b_{MPre}, is also an integer between 1 and m. However, for the simple weighted precedence scheme, the control limit b_{WPre} lies between 1 and $\sum_{k=1}^{j}(n-k+1) = m\left[\frac{n(n+1)}{2} - \frac{(n-j)(n-j+1)}{2}\right] = \frac{mj(2n-j+1)}{2}$. In particular, if $j = r+1$ when n is odd, and $n = 2r+1$, then b_{WPre} lies between 1 and $\frac{m(n+1)(3n+1)}{8}$. Likewise, the control limit b_{WMPre} of the weighted maximal precedence scheme lies between 1 and mn $(= \text{Max}_{1 \le k \le j}\{(n-k+1)m\})$. In this paper, we apply Monte Carlo simulations using R3.2.6 to determine the UCL values as the charting constants, so that $\pi_0(\vartheta) \approx 0.05$ for $\vartheta = 20,\ 25$ and 50. We also verify the results using SAS® v 9.4. To this end, we start a trial value of the charting constant, and generate samples from standard normal distributions for both Phase-I and II, and compute the run-length using the implementation steps given in Subsection 3.1, and replicate the

Table 1. Control limits different schemes for various values of m and n using some standard ϑ values with $\gamma = 0.05$.

Sample sizes		Med scheme			Min scheme			M-pre scheme		
m	n	$\vartheta = 20$	$\vartheta = 25$	$\vartheta = 50$	$\vartheta = 20$	$\vartheta = 25$	$\vartheta = 50$	$\vartheta = 20$	$\vartheta = 25$	$\vartheta = 50$
	5	29	29	30	22	23	24	24	25	26
30	11	27	27	28	14	15	16	17	18	19
	25	25	25	26	8	8	9	8	9	10
	5	48	48	49	36	37	39	39	40	42
50	11	44	45	46	23	23	25	27	28	30
	25	40	41	42	12	13	14	15	16	17
	5	94	95	96	71	72	76	77	78	81
100	11	87	88	89	44	45	48	53	54	57
	25	78	79	81	23	24	26	29	30	32
	5	141	142	144	106	107	114	116	117	122
150	11	129	130	133	64	66	71	78	80	84
	25	116	117	120	34	35	38	42	43	46
	5	281	283	287	210	214	225	229	232	241
300	11	257	260	265	127	130	141	153	156	166
	25	230	232	237	65	67	74	82	85	91
	5	470	471	478	349	356	375	378	385	400
500	11	427	430	440	212	216	234	255	260	275
	25	382	384	393	108	111	122	135	139	149
	5	935	940	953	697	708	749	756	768	800
1000	11	851	858	877	418	431	466	505	517	547
	25	758	765	782	214	219	243	269	275	295
Sample Sizes		W-pre scheme			WM-pre scheme			Rank-sum scheme		
m	n	$\vartheta = 20$	$\vartheta = 25$	$\vartheta = 50$	$\vartheta = 20$	$\vartheta = 25$	$\vartheta = 50$	$\vartheta = 20$	$\vartheta = 25$	$\vartheta = 50$
	5	128	129	133	110	115	120	145	147	150
30	11	244	247	254	165	169	180	322	324	330
	25	492	494	510	238	243	263	856	860	870
	5	209	212	218	180	185	195	229	232	237
50	11	397	401	413	264	268	286	484	488	498
	25	793	801	822	366	375	400	1188	1196	1212
	5	413	417	430	355	361	380	441	444	454
100	11	778	786	809	508	518	550	891	897	916
	25	1538	1553	1594	676	695	745	2017	2028	2060
	5	617	625	641	527	540	568	649	656	671
150	11	1161	1173	1206	749	767	817	1295	1306	1335
	25	2284	2298	2356	982	1008	1083	2841	2858	2906
	5	1230	1241	1279	1054	1073	1128	1280	1292	1324
300	11	2297	2323	2392	1471	1504	1614	2513	2529	2588
	25	4508	4550	4659	1898	1951	2094	5316	5350	5445
	5	2044	2066	2127	1750	1780	1875	2120	2139	2190
500	11	3821	3864	3972	2442	2497	2667	4132	4164	4258
	25	7456	7523	7721	3141	3212	3451	8615	8662	8817
	5	4083	4130	4241	3492	3555	3742	4219	4261	4361
1000	11	7638	7696	7921	4873	4963	5320	8189	8258	8436
	25	14879	14996	15388	6221	6351	6821	16851	16955	17258

same algorithm 50 000 times to observe the simulated run-length distribution, and compute $\pi_0(\vartheta)$. We continue to calibrate the trial value of the charting constant until $\pi_0(\vartheta) \approx 0.05$. More specifically, we reduce the trial value by one if $\pi_0(\vartheta) < 0.05$; otherwise we increase it. For example, when $m = 100$ and $n = 5$, and when the nominal $\pi_0(20) \approx 0.05$, we find that the control limit constants of the traditional Med, Min, and M-Pre schemes are 94, 71, and 77, respectively. Table 1 gives the charting constants of the various schemes discussed in Section 2 for some selected values of (m, n). Table 1 could be handy for practitioners who are designing and implementing precedence-type charting schemes. In Table 1, we also include the charting constant for the Shewhart rank-sum scheme, which is a well-known competitor with the precedence-type schemes.

From Table 1, we observe that the sample size (m, n) affects the values of the charting constants of various schemes to a great extent. From Table 1, we also note that, for a fixed (m, n), when ϑ increases the charting constant of various schemes usually increases; similarly, for any fixed (n, ϑ), the charting constants increase as m increases. Nevertheless, for fixed (m, ϑ), the charting constant increases with n for the W-Pre, WM-Pre, and rank-sum schemes only. For other schemes, we see the opposite phenomenon. For the same design parameters, (m, n, ϑ), $b_{Min} < b_{Med}$, and usually $b_{Med} > b_{MPre}$. During the simulation study, we observe that, for small Phase-I sample sizes, it is difficult to achieve $\pi_0(\vartheta) \approx 0.05$ for the traditional Med scheme. For instance, when $m = 30$, and $\vartheta = 50$, the attained γ of the classic Med scheme is much smaller than 0.05, although $b_{Med} = 30$, which is the maximum value that b_{Med} can take in this case. Thus, $\gamma = 1$ if we consider any $b_{Med} > 30$. The problem happens owing to jumps in the run-length distributions. However, when the Phase-I sample size increases, that problem is solved—and the problem is less severe for the W-Pre scheme.

3.3. In-control robustness

One of the most important advantages of nonparametric schemes over their parametric counterparts is their IC robustness. That is, for fixed (or the same) design parameters, the IC characteristics of the run-length distribution, such as the ARL_0, MRL_0, and PRL_0, remain invariant across all continuous distributions. In this study, we consider a number of distributions:

(i) Standard normal distribution, $N(0,1)$;
(ii) Student's t-distribution, $t(v)$, with degrees of freedom $v = 4$, which is symmetric, but has heavier tails than the normal distribution;
(iii) Gamma distribution, $GAM(3,1)$ and $GAM(1,1)$, which are members of the positively skewed family of densities (note that $GAM(1,1)$ is equivalent to the exponential distribution $EXP(1)$);
(iv) Laplace (or double exponential) distribution, $DEXP(0,1)$, which is also a symmetric distribution with heavier tails than the normal distribution.

We obtain the *UCLs* such that the attained $\pi_0(\vartheta)$ of the schemes under consideration is as close as possible to the pre-specified γ =0.05, and the IC fifth percentile of run-length distribution ϑ (i.e., ϑ_0) values are 20, 25, and 50 under the various distributions mentioned above for different Phase-I sample sizes. Suppose that $(m, n) = (100, 5)$ and that $\vartheta_0 = 25$. Then we observe that the *UCLs* of the M-Pre and WM-Pre schemes are 78 and 361, respectively, regardless of the nature (or shape) of the distribution.

For both unweighted and weighted schemes, regardless of the underlying distribution, the attained ϑ is very close to ϑ_0. It is easy to see that the attained ϑ values of the LPL schemes, under various distributions, are defined by the intervals $\vartheta_0 \pm 0.1\ \vartheta_0$, proving that the LPL charting schemes are IC robust.

Table 2. OOC performance of the proposed monitoring schemes in terms of the 95th *PRL* when $m = 100$ and $n = 5$ for a prescribed ϑ value of 25 under different distributions.

		Monitoring schemes					
Distribution	Shift	Rank-sum	Med	M-Pre	Min	W-Pre	WM-Pre
	0.25	649.78	2479.94	1114.93	725.31	622.79	720.13
	0.50	151.66	570.70	371.35	198.47	148.38	197.15
	1.00	17.61	51.77	49.68	27.72	17.46	27.57
N (0,1)	1.50	4.62	9.75	11.57	7.70	4.57	7.69
	2.00	2.00	3.17	4.41	3.35	2.00	3.31
	3.00	1.00	1.00	1.94	1.17	1.00	1.14
	0.25	467.92	4531.22	718.16	391.58	446.39	393.14
	0.50	72.87	1637.61	132.72	65.18	69.57	65.29
t(3)	1.00	6.21	151.33	10.60	7.67	6.02	7.61
	1.50	2.32	13.16	3.36	3.04	2.0914	3.01
	2.00	2.00	2.24	2.00	2.00	1.98	2.00
	3.00	1.00	1.00	1.06	1.45	1.00	1.05
	0.25	649.48	4470.67	1058.38	579.76	622.07	573.42
	0.50	124.39	1658.33	264.75	98.67	126.60	98.93
DEXP (0,1)	1.00	10.23	211.32	16.63	10.36	10.31	10.34
	1.50	3.14	29.43	5.03	4.15	3.05	4.14
	2.00	2.00	4.93	2.99	2.82	2.00	2.74
	3.00	1.00	1.00	1.96	1.90	1.00	1.78
	0.25	1051.02	4964.04	3947.78	968.91	996.02	973.95
	0.50	306.67	3017.22	1138.38	277.33	287.87	279.11
EXP (1)	1.00	26.51	688.69	92.66	22.40	27.30	22.10
	1.50	3.37	164.79	7.06	1.03	3.92	1.02
	2.00	1.00	41.19	1.00	1.00	1.00	1.00
	3.00	1.00	3.23	1.00	1.00	1.00	1.00
	0.25	955.34	4625.36	2356.32	916.16	907.11	912.14
	0.50	263.89	1920.56	902.62	265.23	254.46	265.67
GAM (1, 3)	1.00	26.91	317.73	86.17	29.99	26.99	30.19
	1.50	4.50	60.00	11.95	5.27	4.78	5.31
	2.00	1.06	13.93	2.78	1.33	1.61	1.33
	3.00	1.00	1.94	1.00	1.00	1.00	1.00

3.4. Out-of-control performance comparison

We have already noted that the LPL schemes considered here are IC robust. Therefore, it is of interest to compare their efficiency when the process is OOC. Tables 2 and 3 display the 95th OOC *PRL* values of various competing schemes when $(m, n) = (100, 5)$ and $(300, 5)$, respectively, for $\vartheta_0 = 25$ under different distributions. For instance, under the $N(0,1)$ distribution, for a pre-specified ϑ_0 value of 25, when $\delta = 0.5$, $m = 100$, and $n = 5$, the M-Pre and WM-Pre charting schemes have a 95% chance to signal on or before the 371st and 197th test samples, respectively. We observe that the W-Pre scheme is the best for detecting small shifts in the location parameter, followed by the rank-sum scheme for the normal distribution. For moderate and large shifts, the W-Pre and rank-sum schemes perform similarly. The Min and WM-Pre schemes outperform the competing schemes under heavier-tailed distributions for small shifts; however, the W-Pre scheme is the best for moderate shifts. We also note that the M-Pre and WM-Pre charting schemes offer a signal on or before the 903rd and 266th samples with a 95% chance in Phase-II under the $GAM(3,1)$ distribution when $\delta = 0.5$ and $(m, n) = (100, 5)$. Here, the W-Pre scheme is more effective. We also observe that under heavier-tailed distributions and significant shifts in the location parameter, the M-Pre and WM-Pre charting schemes may give an OOC signal a bit sooner. For instance, when the underlying IC process distribution is $t(3)$ and the target $\delta = 1.5$, there is a 95% chance

Table 3. OOC performance of the proposed monitoring schemes in terms of the 95th *PRL* when $m = 300$ and $n = 5$ for a pre-specified ϑ value of 25 under different distributions.

		Monitoring schemes					
Distribution	Shift	Rank-sum	Med	M-Pre	Min	W-Pre	WM-Pre
	0.25	391.12	688.69	715.00	466.86	393.09	467.00
	0.50	100.89	189.47	251.00	138.66	102.43	141.00
	1.00	13.95	25.05	38.00	22.60	14.18	23.00
N (0,1)	1.50	4.04	6.27	10.00	6.90	4.03	7.00
	2.00	2.00	2.72	4.00	3.06	2.00	3.00
	3.00	1.00	1.00	2.00	1.07	1.00	1.00
	0.25	259.56	952.02	435.00	245.70	258.55	250.50
	0.50	45.87	282.21	84.00	47.36	45.34	47.00
t(3)	1.00	5.23	23.22	9.00	6.91	5.12	7.00
	1.50	2.07	3.37	3.00	3.01	2.01	3.00
	2.00	2.00	1.12	2.00	2.00	1.96	2.00
	3.00	1.00	1.00	1.00	1.37	1.00	1.00
	0.25	349.11	1072.41	906.50	331.35	355.30	532.00
	0.50	71.70	385.18	349.00	58.36	75.29	160.00
DEXP (0,1)	1.00	7.97	53.03	41.00	9.09	8.00	21.00
	1.50	3.01	8.33	11.00	4.02	3.00	7.00
	2.00	2.00	2.00	4.00	2.68	2.00	3.00
	3.00	1.00	1.00	2.00	1.83	1.00	2.00
	0.25	561.55	1428.20	1947.00	557.54	552.00	557.00
	0.50	160.52	698.95	559.00	158.39	159.23	159.00
EXP (1)	1.00	14.42	167.32	45.00	12.27	15.61	12.00
	1.50	2.02	42.07	3.00	1.00	2.42	1.00
	2.00	1.00	11.35	1.00	1.00	1.00	1.00
	3.00	1.00	1	1.00	1.00	1.00	1.00
	0.25	525.12	1187.50	1327.00	548.28	518.91	553.00
	0.50	153.18	490.75	492.00	167.31	152.81	167.00
GAM (1, 3)	1.00	17.57	90.91	53.00	20.97	18.23	21.00
	1.50	3.30	20.65	8.00	4.09	3.79	4.00
	2.00	1.00	5.97	2.00	1.00	1.00	1.00
	3.00	1.00	1.00	1.00	1.00	1.00	1.00

that the M-Pre and WM-Pre schemes will give an OOC signal on or before the third sample respectively. In contrast, if the underlying IC process follows the GAM(3,1) distribution, for the same shift size there is a 95% chance of observing the OOC signal on or before the 12th and 5th samples, respectively. In Tables 2 and 3, we indicate the best charting scheme with gray shading. In the event that two or more columns are shaded, the competing schemes perform similarly. The summarized findings in Tables 2 and 3 are as follows:

(1) The larger the Phase-I sample size, the more sensitive the proposed scheme.
(2) The smaller the Phase-I sample size, the more unstable and less efficient the proposed scheme.
(3) Under the *N*(0,1) distribution,
  - the W-Pre scheme outperforms all competing schemes for small shifts. However, both the W-Pre and the rank-sum schemes outperform all competing schemes for moderate and large shifts, and
  - the rank-sum scheme outperforms all unweighted competing schemes from small to large shifts. For substantial shifts (i.e. $\delta > 2$), the rank-sum and Med schemes perform similarly.
(4) Under the *t*(3) distribution,

- the Min and WM-Pre schemes outperform all competing schemes for small shifts, and
- for moderate to large shifts, the W-Pre scheme outperforms all competing schemes.

(5) Under the *DEXP*(0,1) distribution,

- for small to moderate shifts, the Min and WM-Pre schemes outperform all competing schemes, and
- for large shifts, the W-Pre and rank-sum schemes outperform all competing schemes.

(6) Under the *EXP*(1) distribution, both the Min and the WM-Pre schemes outperform all competing schemes for small to moderate shifts. For large shifts, they all perform similarly except for the Med scheme, which performs the worst.

(7) Under *GAM*(3,1) distribution,

- the W-Pre scheme outperforms all competing schemes for small to moderate shifts, and
- for moderate to large shifts, the rank-sum scheme outperforms all competing schemes.

(8) The Med scheme is relatively insensitive, regardless of the magnitude of the shift.

The above findings stand, regardless of the Phase-I sample size.

4. Illustrative example

The dataset provided by Sakar et al. (2019) contains information about real-time online shoppers' purchasing intention, and is used to demonstrate the application and implementation of the proposed LPL approach. The dataset consists of several features (or categories)—"Administrative," "Administrative duration," "Informational," "Informational duration," "Product-related," and "Product-related duration"—which represent the number of different pages visited by the user in a session, and the time spent in each of these page categories. The other variables, "Exit rates," "Bounce rates," and "Page value," are Google Analytics metrics for each page on the e-commerce site. For the sake of brevity, we do not go into the detail of each variable. In this example, we only focus on the exit rates and the product-related duration, representing Google Analytics metrics when the user leaves the page and the time spent on the page categories, respectively. When working with data that primarily reflects the time spent on a webpage, it is clear that an upper one-sided chart is desirable. The dataset contains 12 330 sessions; however, we were left with 530 data points by filtering the data. The schemes under consideration are implemented in two phases. In Phase-I, when the process is considered to be IC, we select samples of 300 and 150 observations of the exit rates and the product-related durations respectively; we find the appropriate control limits from Table 1. In Phase-II, we monitor 25 subgroups, each of size 5, for both exit rates and product-related data. We show the plotting statistics of the schemes under consideration, based on "Exit rates" and "Product-related duration" data, in Figures 2

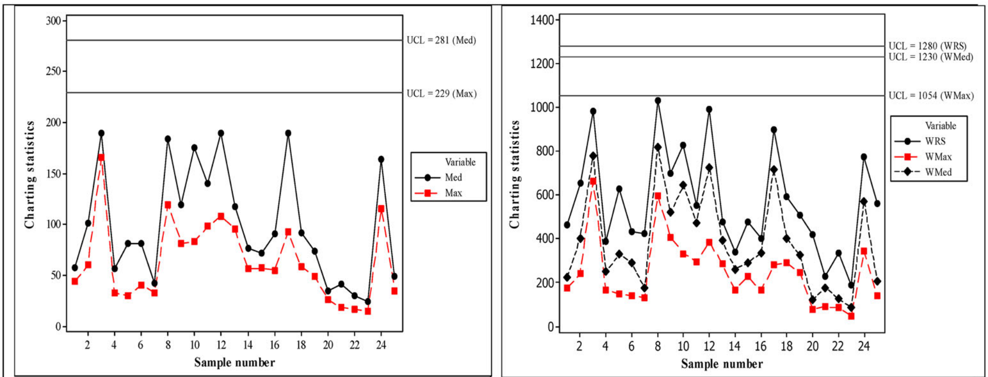

(a) Plotting statistics of the Med and M-Pre charting schemes

(b) Plotting statistics of the Wilcoxon rank-sum, W-Pre and WM-Prec charting schemes

Figure 2. The proposed Rank-sum scheme and precedence-type monitoring schemes for the exit rates data.

and 3, respectively. The Min scheme is not plotted on these figures, as most of the values equal zero, and the Min scheme does not signal.

According to Figure 2, for the exit rate, when $(m, n) = (300, 5)$ with pre-specified ϑ_0 of 20, all five schemes considered here do not give a signal. This is why we consider next another variable—i.e., the "Product-related duration."

According to Figure 3, for the product duration, when $(m, n) = (150, 5)$ with a pre-specified ϑ_0 value of 20, the rank-sum and Med schemes give a signal on the 22nd and 16th subgroups, respectively. However, the M-Pre, WM-Pre and W-Pre schemes do not provide a signal, indicating that the Med scheme performed best, followed by the rank-sum scheme in this situation.

5. Effect of the Phase-I bias

In this section, we study the effect of Phase-I bias on the IC performance of various charting schemes. For brevity and simplicity, we consider Phase-I samples from the standard normal distribution. The actual median in this case is equal to zero. However, in a sample of size m, the observed median might vary. We consider five different classes:

(i) Sample median is less than -0.10, where we have a sizeable downward bias;
(ii) Sample median lies between -0.10 and -0.05, where we have a moderate downward bias;
(iii) Sample median lies between -0.05 and 0.05, where we have a nearly precise estimate;
(iv) Sample median lies between 0.05 and 0.10, where we have a moderate upward bias;
(v) Sample median is more than 0.10, where we have a significant upward bias.

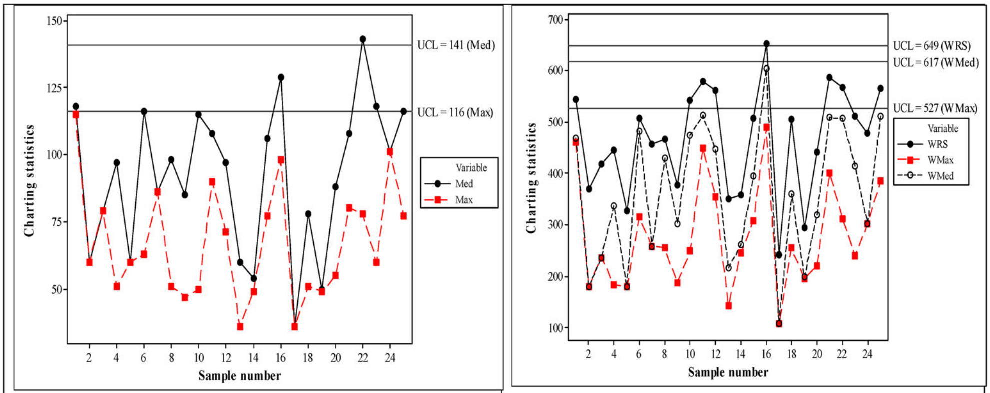

(a) Plotting statistics of the unweighted Med and Max charting schemes

(b) Plotting statistics of the WRS, weighted Med and Max charting schemes

Figure 3. The proposed Rank-sum scheme and precedence-type monitoring schemes for the Product Related Duration data.

Now, with setting $= 5$ and $\vartheta_0 = 25$, we compute the conditional fifth percentile of the run-length for $m = 100, 300,$ and 500 using the control limits in Table 1 for various charting schemes. We study how the conditional fifth percentile values vary for different types of bias, for different types of scheme, and how the values vary as m increases.

In general, we see from Table 4 that the conditional fifth percentile values vary a lot, depending on the Phase-I bias. The conditional fifth percentile values are much lower than the deserving level of 25 for sizeable downward bias, and slightly lower for moderate downward bias. The conditional fifth percentile values are more than the deserving level of 25 when there is sizeable upward bias. For moderate upward bias, the attained value of the fifth percentile is often close to the target, and sometimes higher. When the sample median is very near the population median, as expected, the results are most deserving, except for the cases where we observe jumps; in these instances, the target value of 25 is not precisely achievable.

Overall, from Table 4 we see that the traditional precedence chart and maximal precedence charts are the two least-affected schemes under a Phase-I bias. In contrast, the Min chart is affected heavily by the Phase-I bias, especially with Phase-I sample sizes of less than 300. We can say the same about the W-Pre scheme. The problem does not go away rapidly, even with an increasing reference sample size. However, if the Phase-I bias is minimal, most of these schemes ensure that the attained fifth *PRL* values are closer to the target, even with $m = 100$.

We also study the conditional probability of a false alarm on or before the 25th test sample. We present the results in Table 5, from which we see an inflation of the false alarm probability with a downward bias in the sample median. The rate of inflation reduces as the reference sample size increases. As expected, Table 5 also suggests that the inflation of early false alarm probabilities is minimal for the Med and M-Pre schemes. The Min scheme is again the worst. The effect of Phase-I bias on the WM-Pre and rank-sum schemes is very similar.

Table 4. Conditional 5th *PRL* for various schemes reflecting the effect of Phase-I bias.

Scheme	m	Phase-I Median				
		Less than -0.10	[-0.10, -0.05)	[-0.05, 0.05]	(0.05,0.10]	Greater than 0.10
	100	14	17	21	24	30
Med	300	18	21	24	29	32
	500	18	21	25	28	34
	100	12	17	23	31	49
Min	300	14	19	24	33	43
	500	15	19	25	32	43
	100	16	19	22	25	33
M-Pre	300	18	22	25	31	34
	500	17	21	25	29	31
	100	13	19	25	33	50
W-Pre	300	16	19	25	33	42
	500	15	18	25	33	39
	100	14	21	28	36	54
WM-Pre	300	15	20	26	34	46
	500	16	19	25	31	41
	100	14	20	26	35	55
Rank-sum	300	16	19	25	34	41
	500	16	18	25	32	43

Table 5. Conditional probabilities of a false alarm on or before 25th sample for various schemes.

Scheme	m	Phase-I Median				
		Less than -0.10	[-0.10, -0.05)	[-0.05, 0.05]	(0.05,0.10]	Greater than 0.10
	100	0.0854	0.0718	0.0599	0.0519	0.0417
Med	300	0.0676	0.0610	0.0513	0.0424	0.0409
	500	0.0722	0.0574	0.0488	0.0435	0.0332
	100	0.0990	0.0696	0.0530	0.0388	0.0256
Min	300	0.0824	0.0650	0.0498	0.0372	0.0293
	500	0.0765	0.0645	0.0491	0.0377	0.0262
	100	0.0810	0.0668	0.0556	0.0495	0.0388
M-Pre	300	0.0674	0.0563	0.0483	0.0404	0.0321
	500	0.0739	0.0567	0.0492	0.0412	0.0383
	100	0.0904	0.0661	0.0496	0.0349	0.0271
W-Pre	300	0.0792	0.0640	0.0500	0.0368	0.0285
	500	0.0805	0.6667	0.0499	0.0374	0.0279
	100	0.0840	0.0588	0.0452	0.0325	0.0228
WM-Pre	300	0.0786	0.0630	0.0482	0.0372	0.0259
	500	0.0765	0.0641	0.0491	0.0385	0.0306
	100	0.0873	0.0613	0.0462	0.0352	0.0229
Rank-sum	300	0.0756	0.0640	0.0484	0.0356	0.0309
	500	0.0706	0.0653	0.0488	0.0379	0.0269

6. Summary and recommendations

A large number of studies related to the design and implementation of SPM schemes use the IC *ARL* as the performance metric for the determination of control limits, and consider the OOC *ARL* to compare competing schemes. In general, the run-length distribution of a charting scheme is right-skewed, and even the IC *ARL* may not be finite. Noting this, many researchers have suggested using the *MRL* or any other *PRL*, which provide additional information such as information about early false alarms. In this paper, we discuss the design and implementation of several precedence-type charting schemes, and the rank-sum scheme, using a smaller percentile of the run-length distribution. The determination of the control limit using the lower percentile point of the run-length distribution is easier and faster than the determination of control limits based on the *ARL*. Also, the use of the lower percentile restricts the probability of early false alarms to a prefixed level.

We compare the performance of six distribution-free SPM schemes for location shift, using a high *PRL* value. In respect of the 95th OOC *PRL* values, the weighted precedence-type schemes outperform the unweighted precedence-type schemes. However, we notice that these schemes might be more affected in the presence of sizeable upward or downward bias in the reference sample median. In contrast, the Med and M-Pre schemes are less affected by considerable bias in the reference sample. It is not easy to choose between the various competing schemes. However, we feel that the Min chart may be disregarded.

We advise operators and practitioners to apply distribution-free schemes when they do not have any knowledge of the underlying process distribution. In particular, to detect a location shift, they could use the W-Pre or the WM-Pre scheme if the Phase-I sample is well established. If there is some doubt about possible downward bias, it is safer to use the Med scheme or the M-Pre scheme. However, more exploration is required on the overall performances of various schemes, the performance of the individual schemes, and the effect of Phase-I bias after omitting a few observations of reference samples with extreme ranks. We recommend the design and comparison of various other existing charting schemes using the PRL-based methods used in this paper.

Funding

Marien Graham's research was funded by the National Research Foundation (NRF) [Reference: CSRP190415430728, Grant number: 120401].

ORCID

Jean-Claude Malela-Majika http://orcid.org/0000-0001-7236-7678
Marien A. Graham http://orcid.org/0000-0003-4071-9864

References

Balakrishnan, N, and R. Frattina. 2000. Precedence test and maximal precedence test. In *Recent advances in reliability theory*, 355–78. Boston, MA: Birkhäuser. doi:10.1007/978-1-4612-1384-0_23.

Balakrishnan, N, and H. K. T. Ng. 2001. A general maximal precedence test. In *system and bayesian reliability: Essays in honor of Prof. Richard E. Barlow on His 70th Birthday*, ed. Y. Hayakawa, T. Irony, and M. Xie, 105–22. Singapore: World Scientific. doi:10.1142/9789812799548_0007.

Balakrishnan, N, and H. K. T. Ng. 2006. *Precedence-type tests and applications*. Hoboken, New Jersey: John Wiley & Sons.

Balakrishnan, N., C. Paroissin, and J. C. Turlot. 2015. One-sided control charts based on precedence and weighted precedence statistics. *Quality and Reliability Engineering International* 31 (1):113–34. doi:10.1002/qre.1750.

Čampulová, M., P. Veselík, and J. Michálek. 2017. Control chart and six sigma based algorithms for identification of outliers in experimental data, with an application to particulate matter PM10. *Atmospheric Pollution Research* 8 (4):700–8. doi:10.1016/j.apr.2017.01.004.

Chakraborti, S. 2007. Run length distribution and percentiles: The Shewhart chart with unknown parameters. *Quality Engineering* 19 (2):119–27. doi:10.1080/08982110701276653.

Chakraborti, S, and M. A. Graham. 2019b. *Nonparametric statistical process control*. New York: NY, USA: John Wiley & Sons.

Chakraborti, S., and M. A. Graham. 2019a. Nonparametric (distribution-free) control charts: An updated overview and some results. *Quality Engineering* 31 (4):523–44. doi:10.1080/08982112.2018.1549330.

Chakraborti, S., P. Laan, and M. A. Wiel. 2004. A class of distribution-free control charts. *Journal of the Royal Statistical Society: Series C (Applied Statistics)* 53 (3):443–62. doi:10.1111/j.1467-9876.2004.0d489.x.

Chen, H., and C. Huang. 2014. The use of a CUSUM residual chart to monitor respiratory syndromic data. *IIE Transactions* 46 (8):790–7. doi:10.1080/0740817X.2012.761369.

Faraz, A., E. Saniga, and D. Montgomery. 2019. Percentile-based control chart design with an application to Shewhart $\overline{X}$ and S^2 control charts. *Quality and Reliability Engineering International* 35 (1):116–26. doi:10.1002/qre.2384.

Graham, M. A., A. Mukherjee, and S. Chakraborti. 2012. Distribution-free exponentially weighted moving average control charts for monitoring unknown location. *Computational Statistics & Data Analysis* 56 (8):2539–61. doi:10.1016/j.csda.2012.02.010.

Jensen, W. A., L. A. Jones-Farmer, C. W. Champ, and W. H. Woodall. 2006. Effects of parameter estimation on control chart properties: A literature review. *Journal of Quality Technology* 38 (4):349–64. doi:10.1080/00224065.2006.11918623.

Koutras, M. V, and I. S. Triantafyllou. 2020. Recent advances on univariate distribution-free shewhart-type control charts. In *Distribution-free methods for statistical process monitoring and control*, 1–56. Cham: Springer.

Kumar, N., and A. Baranwal. 2019. Design and implementation of qth quantile-unbiased tr-chart for monitoring times between events. *Quality and Reliability Engineering International* 35 (4): 1061–80. doi:10.1002/qre.2445.

Li, J., K. Liu, and X. Xian. 2017. Causation-based process monitoring and diagnosis for multivariate categorical processes. *IISE Transactions* 49 (3):332–43. doi:10.1080/0740817X.2016.1241455.

Li, J., and P. Qiu. 2016. Nonparametric dynamic screening system for monitoring correlated longitudinal data. *IIE Transactions* 48 (8):772–86. doi:10.1080/0740817X.2016.1146423.

Malela-Majika, J. C., E. M. Rapoo, A. Mukherjee, and M. A. Graham. 2020. Distribution-free precedence schemes with a generalized runs-rule for monitoring unknown location. *Communications in Statistics-Theory and Methods* 49 (20):4996–5027. doi:10.1080/03610926.2019.1612914.

Malela-Majika, J. C., S. C. Shongwe, and P. Castagliola. 2022. One-sided precedence monitoring schemes for unknown shift sizes using generalized 2-of-(h + 1) and w-of-w improved runs-rules. *Communication in Statistics- Theory and Methods* 51 (9):2803–37. doi:10.1080/03610926.2020.1780448.

Mukherjee, A., M. A. Graham, and S. Chakraborti. 2013. Distribution-free exceedance CUSUM control charts for location. *Communications in Statistics - Simulation and Computation* 42 (5): 1153–87. doi:10.1080/03610918.2012.661638.

Mukherjee, A., and R. Sen. 2015. Comparisons of Shewhart-type rank based control charts for monitoring location parameters of univariate processes. *International Journal of Production Research* 53 (14):4414–45. doi:10.1080/00207543.2015.1012605.

Mukherjee, A., and R. Sen. 2018. Optimal design of Shewhart-Lepage type schemes and its application in monitoring service quality. *European Journal of Operational Research* 266 (1):147–67. doi:10.1016/j.ejor.2017.09.013.

Ng, H. K. T., and N. Balakrishnan. 2005. Weighted precedence and maximal precedence tests and an extension to progressive censoring. *Journal of Statistical Planning and Inference* 135 (1):197–221. doi:10.1016/j.jspi.2005.02.014.

Sakar, C. O., S. O. Polat, M. Katircioglu, and Y. Kastro. 2019. Real-time prediction of online shoppers' purchasing intention using multilayer perceptron and LSTM recurrent neural networks. *Neural Computing and Applications* 31 (10):6893–908. doi:10.1007/s00521-018-3523-0.

Song, Z., A. Mukherjee, Y. Liu, and J. Zhang. 2019. Optimizing joint location-scale monitoring–An adaptive distribution-free approach with minimal loss of information. *European Journal of Operational Research* 274 (3):1019–36. doi:10.1016/j.ejor.2018.11.060.

Van der Laan, P., and S. Chakraborti. 2001. Precedence tests and Lehmann alternatives. *Statistical Papers* 42 (3):301–12. doi:10.1007/s003620100060.

Woodall, W. H., M. J. Zhao, K. Paynabar, R. Sparks, and J. D. Wilson. 2017. An overview and perspective on social network monitoring. *IISE Transactions* 49 (3):354–65. doi:10.1080/0740817X.2016.1213468.